Journal Pre-proofs

Application of $MnFe_2O_4$ and AuNPs Modified CPE as a Sensitive Flunitrazepam Electrochemical Sensor

Bahman Mohammadian Asiabar, Mohammad Ali Karimi, Hossein Tavallali, Mehdi Rahimi-Nasrabadi

PII: S0026-265X(20)32714-4
DOI: https://doi.org/10.1016/j.microc.2020.105745
Reference: MICROC 105745

To appear in: *Microchemical Journal*

Received Date: 18 August 2020
Revised Date: 25 September 2020
Accepted Date: 9 November 2020

Please cite this article as: B.M. Asiabar, M.A. Karimi, H. Tavallali, M. Rahimi-Nasrabadi, Application of $MnFe_2O_4$ and AuNPs Modified CPE as a Sensitive Flunitrazepam Electrochemical Sensor, *Microchemical Journal* (2020), doi: https://doi.org/10.1016/j.microc.2020.105745

Application of $MnFe_2O_4$ and AuNPs Modified CPE as a Sensitive Flunitrazepam Electrochemical Sensor

Bahman Mohammadian Asiabar[1, 2], Mohammad Ali Karimi[1], Hossein Tavallali[1], Mehdi Rahimi-Nasrabadi[3, 4*]

[1]*Department of chemistry, Payame Noor University, 19395-4697 Tehran, Iran*

[2]*Department of Chemistry, Faculty of Science, Imam Ali University, Tehran, Iran*

[3]*Chemical Injuries Research Center, Systems Biology and Poisonings Institute, Baqiyatallah University of Medical Sciences, Tehran, Iran*

[4]*Faculty of Pharmacy, Baqiyatallah University of Medical Sciences, Tehran, Iran*

Correspond authors:

M. Rahimi Nasrabadi; Email: rahiminasrabadi@gmail.com, Tel: +98 21 82483409

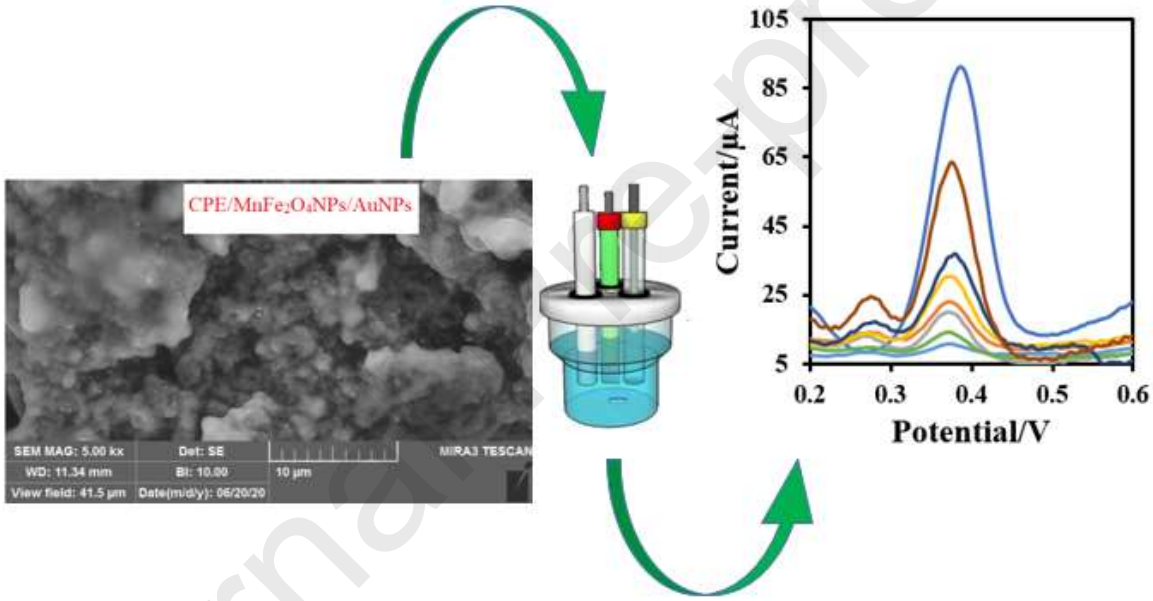

Graphical Abstract

Abstract

Flunitrazepam or Rohypnol belongs to the group of benzodiazepines (Schedule IV) with much higher and long-lasting effects on the nervous system. They are also used in suicide and aggression. Since it can eventually be detected in the urine within 72 h, it is important to measure it in the biological fluids quickly and accurately. The $MnFe_2O_4$ was synthesized through the sol-gel method and used in the modification of the carbon paste electrode (CPE) beside AuNPs. The clever utilization of the $MnFe_2O_4$ and AuNPs in the CPE provided excellent properties such as high surface area and current amplification through embedding a fantastic sensing interface for high selective electrochemical measuring of the flunitrazepam. In the optimized experimental conditions, the anodic current related to the oxidation of the flunitrazepam onto the sensor surface at 0.41 V presented a linear response towards the concentrations of the flunitrazepam at a range of 0.1-100 μM. The detection limit (LOD) was founded to be 0.33 μM. The applicability of the sensor was evaluated during the flunitrazepam determination in the presence of some mineral ions and organic compounds. Furthermore, the developed sensor has been used successfully for measuring flunitrazepam in human plasma samples. These findings reflect the strategy based on the CPE as a cost-effective platform may economically create a promising candidate for the practical determination of the flunitrazepam in the rutin clinical testing.

Key Word: Flunitrazepam, $MnFe_2O_4$, AuNPs, Electrochemical sensors

1. Introduction

Flunitrazepam or Rohypnol is owned to benzodiazepines and is an anesthetic and hypnotic drug which lawfully recommended in some countries for the treatment of severe insomnia (sleeping disorders) [1, 2]. The sedative effects of both alcohol and flunitrazepam (as sedative medication) can enhance each other which causes spiritual and motor disorders and causes the victim to become "silent." It is a short-term forgetfulness that prevents the victim from remembering. Flunitrazepam as a psychotropic drug was frequently associated with drug-facilitated sexual assault [3]. Based on the mentioned reasons, developing a sensitive analytical method for the determination of flunitrazepam in various samples is necessary. Up to date, numerous analytical techniques such as desorption electrospray ionization mass spectrometry [4], fluorescence spectroscopy [5], capillary electrophoresis [6], liquid and gas chromatography [7-10] have been utilized for measurement of flunitrazepam. High cost, complexity, insufficient sensitivity, and time-consuming are some practical drawbacks of these traditional methods. Despite considerable progress, there are still challenges in applying a reliable method for sensitive and selective analysis of flunitrazepam. Considering some advantages such as simplicity, suitable cost, easy operation, high sensitivity, low limit of detection (LOD), and fast response, electrochemical detection methods have lately been employed for this aim [11, 12].

Because of the slow rate of electrochemical reactions at the surface of traditional electrodes and the high overpotential required to induce these reactions, modification of bare electrode with different kinds of nanomaterials is necessary to achieve high selectivity and sensitivity [13-20].

Nanomaterials have advantages due to their unique size and physical characteristics [21-27]. Until now, various electroanalytical methods based on carbon-based working electrodes like carbon paste, screen printed and glassy carbon electrode have been reported for measurement of flunitrazepam [28-30]. However, the carbon paste electrode (CPE) has attracted high attention in

electrochemistry due to its non-toxic nature, eco-friendly, low-cost, easy preparation, broad operational potential window, easy chemical, and mechanical modification, and renewable surface [31]. Among the various nanomaterials, nanoparticles of manganese (II) ferrite bimetallic oxides ($MnFe_2O_4$), have attracted the attention of researchers in recent decades due to having good features like low cost, eco-friendly, and wide source of raw materials [32, 33]. However, the poor electrochemical performance of these nanomaterials, which are due to limitations such as low electrical conductivity, fast aggregation, and expansion associated with the charging-discharging process, limit their single-use in the manufacture of electrochemical sensors. Hence, fabrication of $MnFe_2O_4$ based-various nanocomposites through the coupling of $MnFe_2O_4$ with different mediators such as carbon nanomaterials [34], metal nanoparticles [35], and organic ligands [36] can lead to the creation of appropriate features in the bimetallic oxides.

Having unique features including great specific surface area (due to large surface to volume ratio), biological compatibility, good electrocatalytic properties, exceptional heat and electrical conductivity, and high stability, Au nanoparticles attracted the attention of researchers for the fabrication of electrochemical sensors [37-41]. Synthetic of gold nanoparticles (AuNPs) by different techniques can produce nanoparticles with various shapes (like spheres, cubes, rods, nanowires, and triangles) [42-46]. Recently, plentiful applications in the various sciences such as chemistry, physics, catalysis, medicine, electrochemical sensors, etc. have been reported for Au based-nanomaterials [47, 48]. AuNPs can be used in the role of catalyst for facilitating electron transfer between the electrode surface and electro-active species which finally can cause to increase in the rate of electrochemical reactions [49]. Therefore, the combination of AuNPs with the other nanomaterials such as conductive polymers, carbon nanostructures, metal nanoparticles,

and metal oxides can lead to improved electrocatalytic attributes, active sites, sensitivity, and detection limit of the electrochemical sensors.

The objective of the present research is the fabrication of a new sensor by modification of a carbon paste electrode with two components ($MnFe_2O_4$ and AuNPs) for determination of the flunitrazepam. For this purpose, at the first, the carbon paste electrode was modified with $MnFe_2O_4$ and then the AuNPs were deposited on the surface of MnFe2O4 by an electrochemical deposition method.

2- Experimental

2-1-Chemicals and Apparatus

Phosphoric acid, manganese nitrate, acetic acid, iron nitrate, $HAuCl_4\ 3H_2O$, potassium carbonate, ethylene glycol, iron chloride, potassium ferricyanide/ferrocyanide, boric acid, flunitrazepam sodium hydroxide, and copper sulfate were taken from Merck. Britton–Robinson (BR) buffer solution (0.04M) which was used for electrochemical experiments were prepared in double-distilled water and the pH was adjusted by hydrochloric acid and sodium hydroxide.

Voltammetric testing was performed using a three-electrode system consisting of the Ag/AgCl electrode as the reference electrode (Azar electrode Co, Iran), the platinum wire as the auxiliary electrode (Azar electrode Co, Iran), and unmodified and modified CPE as the working electrode. The palm sense EM State series was employed to perform the square- wave voltammetry (SWV), cyclic voltammetry (CV), and EIS analyses. To the investigation of the morphology of $MnFe_2O_4$ nanoparticles and modified electrode, FESEM images were obtained using MIRA3 TESCAN field emission scanning electron microscope coupled with an EDS test.

2-2- Preparation of $MnFe_2O_4$ nanoparticles

The $MnFe_2O_4$ was synthesized through the sol-gel technique according to the method previously reported in the literature [48]. Briefly, iron nitrate and manganese nitrate (with a molar

ratio of 2:1) were dissolved in ethylene glycol at about 40 °C. The sol of the metal compounds was heated to around 60 °C until a wet gel is produced. The desired product was obtained by drying the obtained gel at about 100 °C self-ignites.

2-3- Fabrication of working electrode

The $MnFe_2O_4$/CPE and CPE were prepared according to the following procedure. 0.14 g of graphite, 0.01g of $MnFe_2O_4$, and some oil were mixed to achieve a uniform paste. The resulting paste was then put into a plastic tube (id= 2 mm). The electrical transmission was made using a copper wire. The surface of the electrode was polished on a polish sheet to be perfectly uniform and was subsequently washed with distilled water. The unmodified CPE was obtained from a mixture of 0.15 g of graphite and oil with no modifier similar to the mentioned procedure.

The AuNPs were formed onto the $MnFe_2O_4$/CPE surface by electrodeposition of $HAuCl_4$ $3H_2O$. The electrodeposition step was done in a 5 mM solution of $HAuCl_4.3H_2O$ containing 0.1 M KCl through 10 consecutive CV scans in the potential range of 0.2 to -0.1 V at the scan rate of 50 mV/s [51].

3. Results and discussion Characterization

3.1 Investigation of physico-chemical features of $MnFe_2O_4$NPs

The FESEM and EDS techniques were used to study the morphology of the CPE, CPE/$MnFe_2O_4$NPs, and CPE/$MnFe_2O_4$NPs/AuNPs surfaces. Figure 1 (a to c) shows the FE-SEM images of the CPE, CPE/$MnFe_2O_4$NPs, and CPE/$MnFe_2O_4$NPs/AuNPs surface. The FE-SEM image indicates a nanostructure layer of the AuNPs onto the modified CPE/$MnFe_2O_4$NPs surface. The FE-SEM image of $MnFe_2O_4$NPs shows Cubic (Figure 1d) which well illustrates the successful synthesis of nanoparticles. Also, the presence of different elements into the CPE was analyzed

with the EDS technique. Figure 1d confirms the presence of the C, Mn, Fe, O and Au on the modified electrode. Also, the weight percent of each element is listed in the inset.

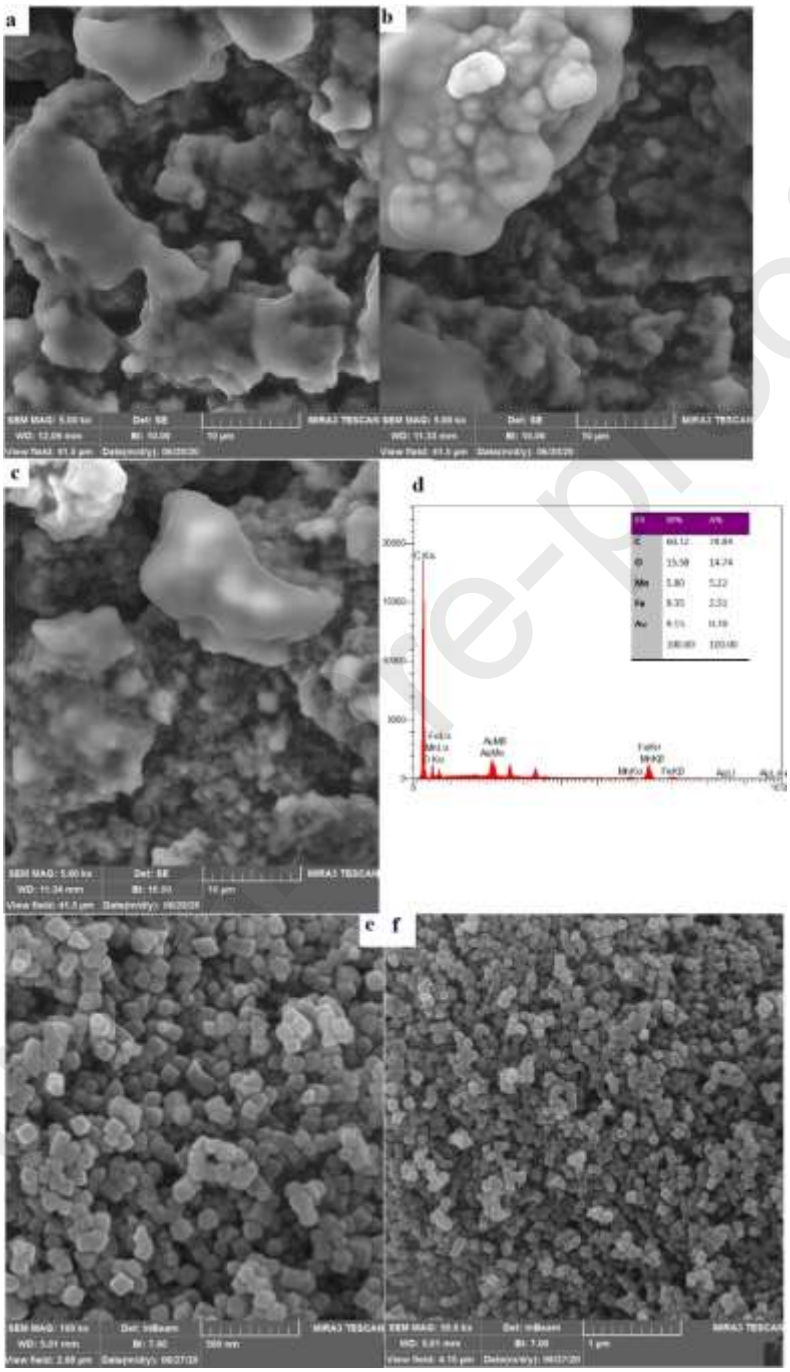

Figure 1 The FE-SEM images of the (a) CPE, (b) CPE/$MnFe_2O_4$NPs, (c) CPE/$MnFe_2O_4$NPs/AuNPs and (d) the corresponding EDS spectrum of the synthesized CPE/$MnFe_2O_4$NPs/AuNPs, The FE-SEM images of the $MnFe_2O_4$NPs

The XRD pattern of $MnFe_2O_4$ nanostructure (which has a cubic geometry) prepared by the sol-gel method is illustrated in Figure 2. As it is shown, the obtained composition is pure and no impurities such as FeO is observed. The peak broadening can be proven nanocrystalline nature of the synthesized samples. The XRD patterns were in agreement with JCPDS data (number 74 - 2403). The average dimensions of the $MnFe_2O_4$ samples were determined using the Scherrer equation and the full width at half-maximum data of all phases present in the sample peaks.

$$D=\frac{K\lambda}{\beta cos\theta} \qquad \text{Scherrer equation}$$

where k=0.9, the X-ray radiation wavelength λ was 0.154056 nm, β expresses the corrected full width at half-maximum after eliminating instrumental broadening, and θ represents Bragg's angle. The results show that the average crystal size is 35.5 nm (Table1).

Table 1. Crystallite size of the $MnFe_2O_4$ samples

No.	B obs.[˚2th]	B std.[˚2th]	Peak pos. [˚2th]	B struct. [˚2th]	Crystallite size (nm)
1	0.236	0.09	33.02	0.146	35.53

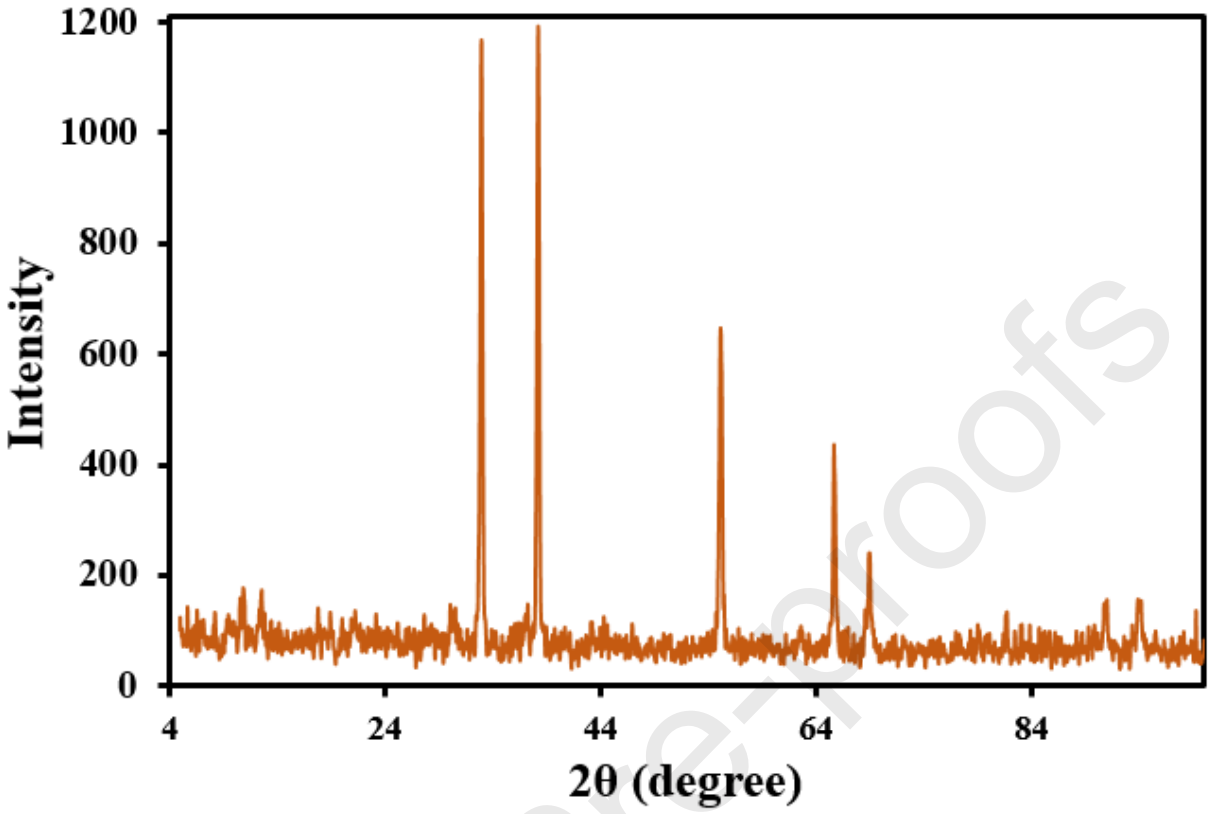

Figure 2. XRD pattern of $MnFe_2O_4$NPs

The FT-IR spectra can reflect the functional groups of as-synthesized $MnFe_2O_4$NPs (Figure 3). The observed strong absorption peak at 3400 cm^{-1} is related to O-H of adsorbed water on the surface of nanoparticles [50, 51] The band at 477 cm^{-1} corresponds to the Fe-O stretching vibration. The bands at 1700 to 1500 cm^{-1} are related to the ethylene glycol CH_2 stretch bond (physically adsorbed).

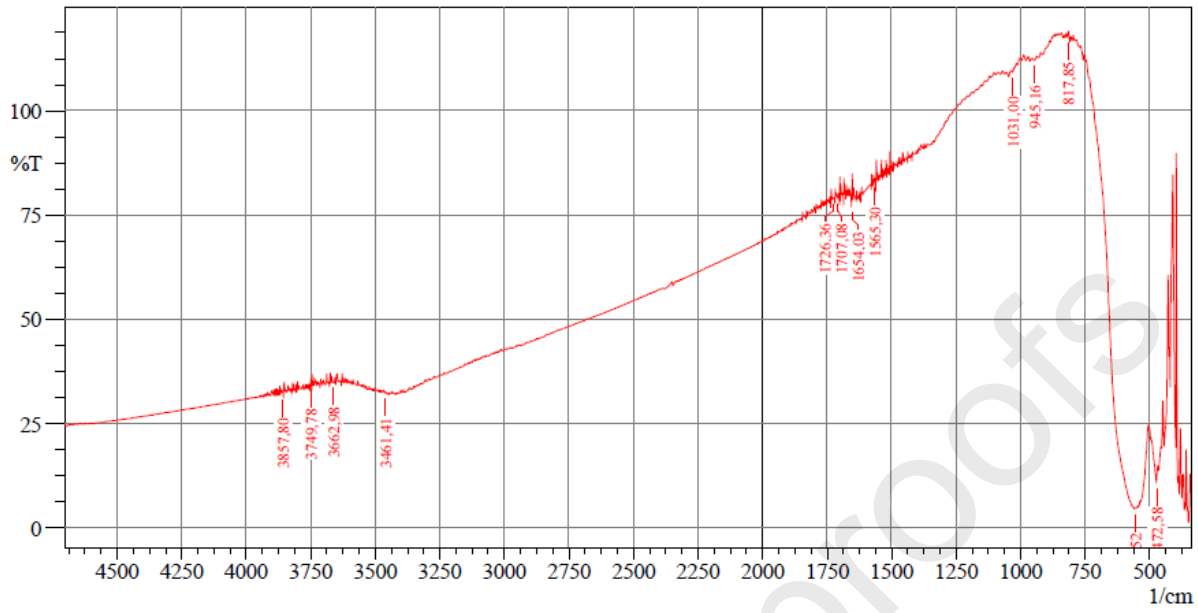

Figure 3. FTIR spectra of $MnFe_2O_4$NPs

3.2 Electrochemical studies of CPE, CPE/$MnFe_2O_4$NPs and CPE/$MnFe_2O_4$NPs/AuNPs

The electrochemical behavior of the CPE, CPE/$MnFe_2O_4$NPs, and CPE/$MnFe_2O_4$NPs/AuNPs was studied by the CV technique in the 0.1 M KCl containing 1 mM $[Fe(CN)_6]^{3-/4-}$ as the redox probe at a scan rate of 50 mV s^{-1} (Figure 4a). As shown in Figure 4a, in comparison to the bare CPE, CPE/$MnFe_2O_4$NPs, the CPE/$MnFe_2O_4$NPs/AuNPs presents a well-defined reversible redox peak with a higher current signal. The peak to peak separation potential (ΔE_p) value for bare CPE, CPE/$MnFe_2O_4$NPs, and CPE/$MnFe_2O_4$NPs/AuNPs were obtained to be 250, 190, and 70 mV, respectively. This decrease of the ΔE_p value and the increase of the current signal in the modified electrode can be attributed to utilizing the $MnFe_2O_4$NPs and AuNPs as an efficient modifiers in the modification process.

The EIS technique was used to evaluate electrochemical impedance behavior of the CPE, CPE/$MnFe_2O_4$NPs and CPE/$MnFe_2O_4$NPs/AuNPs in a solution containing 1 mM of $[Fe(CN)_6]^{3-/4-}$ and 0.1 mol L^{-1} KCl in a range of 0.1 Hz to 50 kHz (Figure 4b). As presented in the Nyquist plot

in Figure 4, a large semicircle is observed for the bare CPE at high frequencies indicating the high resistance of mass transfer (R_{ct}) due to the decrease in the charge and mass transfer rates at the electrode surface [54-56]. The R_{ct} values of the CPE/$MnFe_2O_4$NPs (R_{ct} =0.850 kΩ) and CPE/$MnFe_2O_4$NPs/AuNPs (R_{ct} = 0.005 kΩ) were smaller than the bare CPE (R_{ct} = 1.500 kΩ). In fact, the presence of the $MnFe_2O_4$NPs and AuNPs as a modifier in the electrode modifying process leads to increase electron transfer kinetic onto the electrode surface and lower R_{ct} value. A significant decrease in the R_{ct} value was observed in the modified electrode with a mixture of the $MnFe_2O_4$NPs and AuNPs as the nanocomposite (CPE/$MnFe_2O_4$NPs/AuNPs, R_{ct} =0.005 kΩ), indicating a high conductivity of the nanocomposite in the CPE. The obtained EIS results certified the successful fabrication of the sensor.

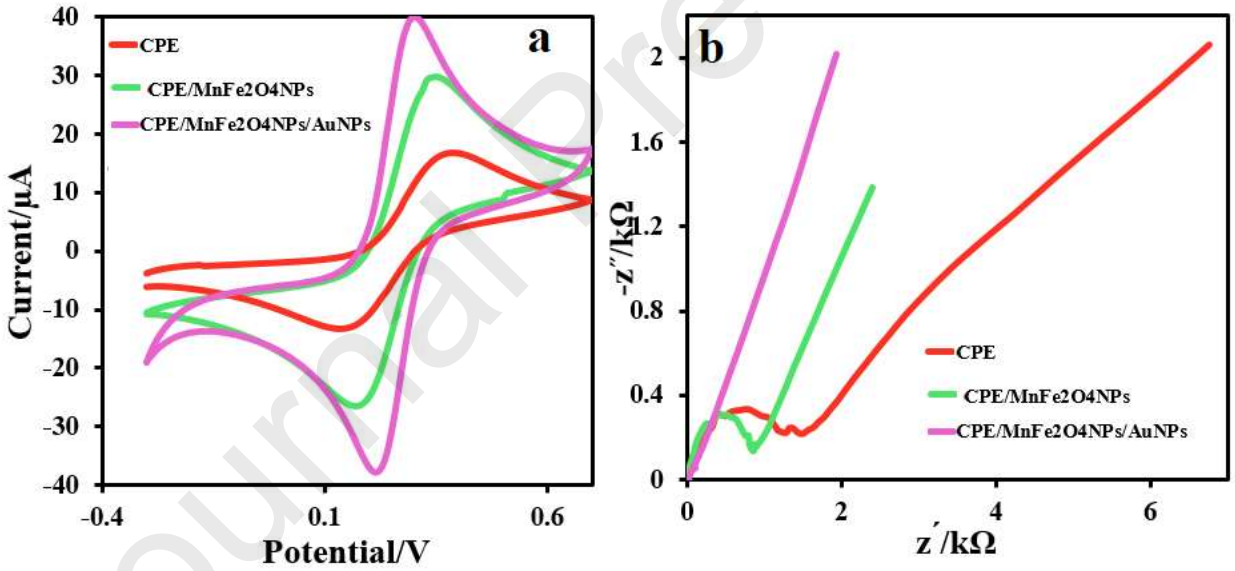

Figure 4 (a) the recorded CVs of the CPE, CPE/$MnFe_2O_4$NPs and CPE/$MnFe_2O_4$NPs/AuNPs in the same redox probe at the scan rate of 50 mV s^{-1}. (b)The recorded Nyquist plots of different CPE, CPE/$MnFe_2O_4$NPs and CPE/$MnFe_2O_4$NPs/AuNPs in a solution containing 1 mM $[Fe(CN)_6]^{3-/4-}$ as the redox probe and 0.1 mol L^{-1} KCl in a range of 0.1 Hz to 50 kHz

To more study, the CV curves related to the surface of the CPE, CPE/$MnFe_2O_4$NPs and CPE/$MnFe_2O_4$NPs/AuNPs in the absence and presence of the 25 µM flunitrazepam in 0.04 M BR (pH= 8.0) were recorded (Figure 5). An oxidation peak at 0.41 V vs. Ag/AgCl with a peak current of 2.54 µA for the CPE was achieved. In contrast, an irreversible oxidation peak with a little positive potential than the bare CPE with higher current was recorded for the CPE/$MnFe_2O_4$NPs (7 µA) and CPE/$MnFe_2O_4$NPs/AuNPs (10 µA). The considerable increase in the oxidation peak current of the flunitrazepam on the CPE/$MnFe_2O_4$NPs/AuNPs surface can be attributed to the presence of the $MnFe_2O_4$NPs and AuNPs as the useful modifier in the modification process.

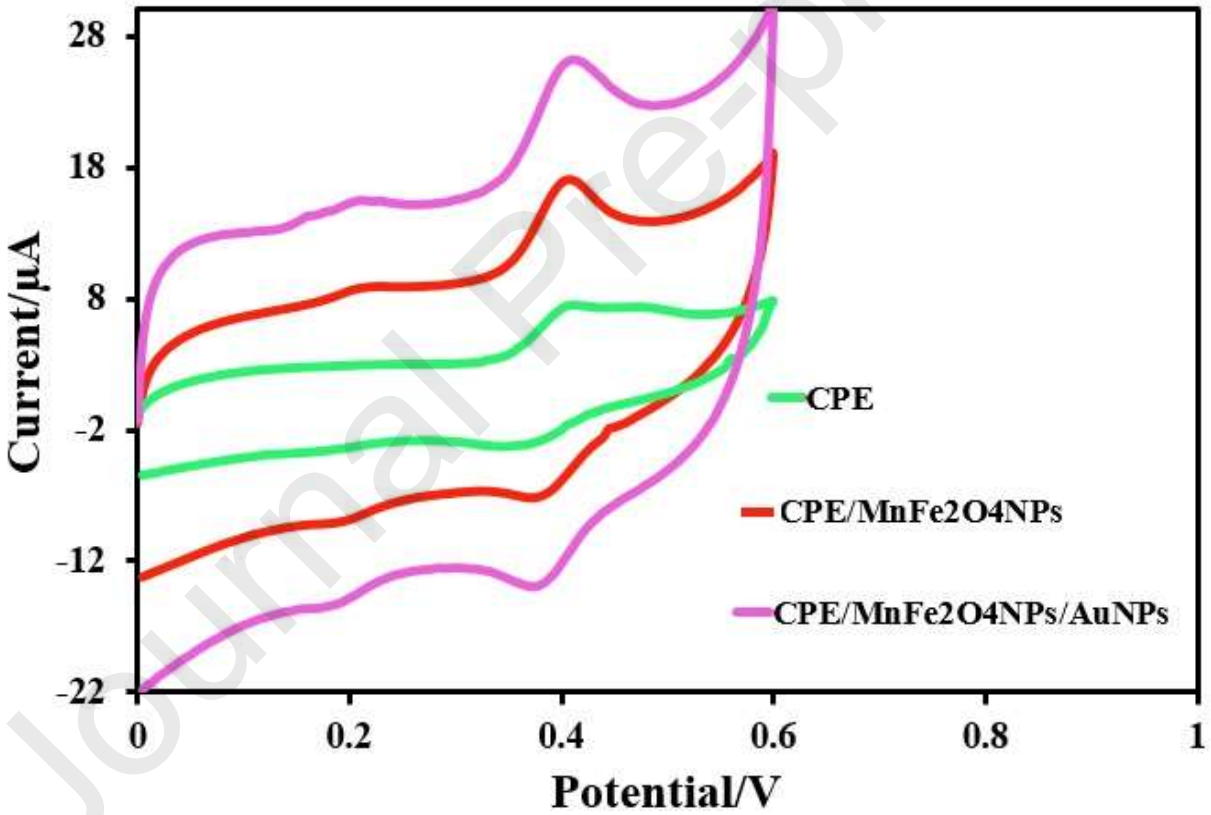

Figure 5. The recorded CVs of the CPE, CPE/$MnFe_2O_4$NPs and CPE/$MnFe_2O_4$NPs/AuNPs in the presence of 25 µM flunitrazepam in 0.04 M BR (pH= 8.0) at a scan rate of 50 mV s^{-1}.

CV curves related to the CPE/$MnFe_2O_4$NPs/AuNPs surface were recorded in 0.04 M BR containing 25 μM flunitrazepam at a pH range of 4.0-8.0 with a scan rate of 50 mV s^{-1} (Figure 6a), to study the pH effect of the solution. According to Figure 6a, the peak current decreases by increasing the pH value indicating a negative shift in the peak potential. As can be seen, the pH value of 8.0 presents the maximum current response, so this value has been selected as the optimum ones for further experiments. Also, **Figure 6b** displays a dependence of oxidation peak potential (E_p) of the flunitrazepam versus pH value with an excellent linear relationship under an equation of E_p (V) = –0.045 pH + 0.7333 (R^2 = 0.9871). According to the equation, a slope of –0.045 V/pH, which is close to the Nernst value of 59 mV was observed, indicating an equal number of electron and proton involved in the electrooxidation process of flunitrazepam onto the CPE/$MnFe_2O_4$NPs/AuNPs surface. CVs of the CPE/$MnFe_2O_4$NPs/AuNPs surface at different scan rates under a range of 10-300 mV s^{-1} were recorded to check the influence of the scan rate on the electrooxidation current response (Figure 6c). The results indicated that the E_p value was slightly shifted to positive values with increasing the scan rate. This behavior confirms the kinetic limitation for the electrooxidation of flunitrazepam onto the CPE/$MnFe_2O_4$NPs/AuNPs surface. The linear relationship between I_p and $v^{1/2}$ under an equation of $I_p = 0.84\ v^{1/2}$-0.633 (R^2 = 0.9922) (Figure 6d) suggests a diffusion-controlled process for flunitrazepam on the CPE/$MnFe_2O_4$NPs/AuNPs surface.

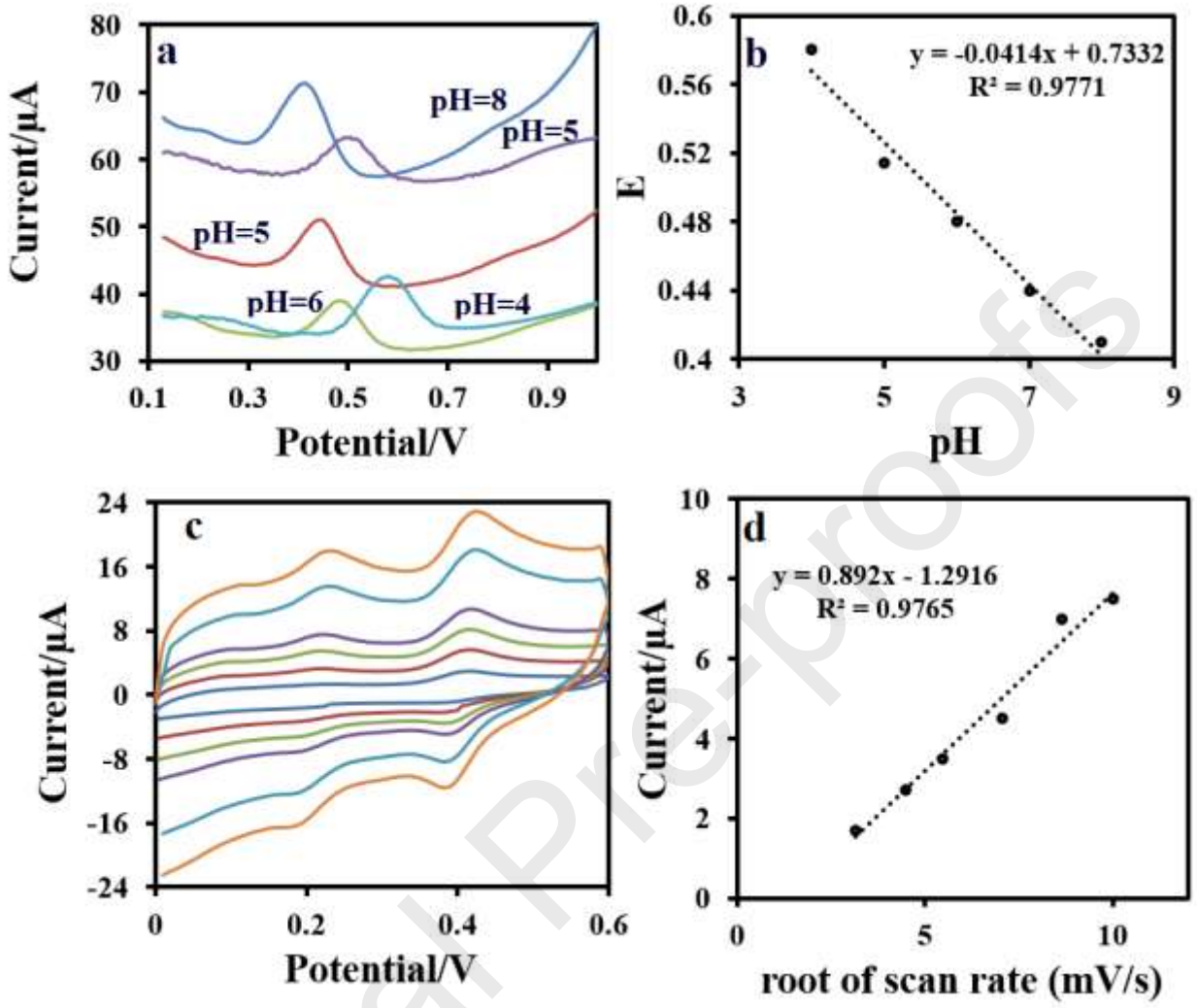

Figure 6. (a) DPVs of the CPE/$MnFe_2O_4$NPs/AuNPs in various pH values (4, 5, 6, 7, and 8). (b) E_p vs. pH value in the presence of 25 µM flunitrazepam. (c) CVs in 0.04 M BR (pH=8.0) containing 25 µM flunitrazepam solution at different scan rates (10-100 mVs^{-1}) and (d) the plot of I_p vs. $\upsilon^{1/2}$.

To certify the analytical applicability of the flunitrazepam sensor, the DPV technique was employed in different concentrations of the target in 0.04 M BRB with pH = 8 (Figure 7). It was found that a significant increase in the DPV signals was created by increasing the flunitrazepam concentration in the range of 0.1-90 µM. Based on the obtained regression equation of y = 0.7518

x + 4.5915 with a correlation coefficient of 0.9893, the limit of detection (LOD) was estimated to be 0.33 µM. As presented in Table 1, the applied strategy has admirable properties in comparison with other reported methods in flunitrazepam detection. These satisfactory results may be ascribed to the targeted utilization of the CPE/$MnFe_2O_4$NPs/AuNPs in embedding an efficient platform for flunitrazepam sensing.

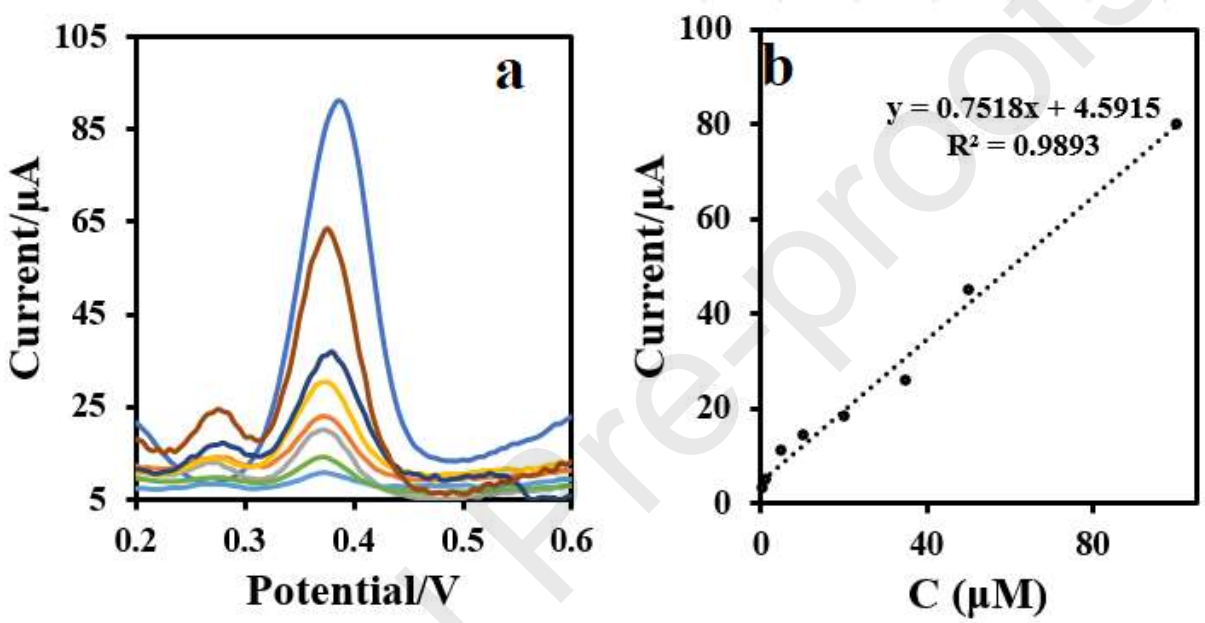

Figure 7 (a) The recorded DPVs for different concentrations of flunitrazepam from 0.1-100 µM on the CPE/$MnFe_2O_4$NPs/AuNPs in 0.04 mol L^{-1} BRB (pH= 8) and (b) the relative calibration curve.

Table 1. Comparison of the analytical parameters of the strategy for flunitrazepam detection with other reported methods.

Electrode	Linear rang (μM)	LOD (nM)	Ref.
SPGE	3.19-30.40	1.5	[11]
SPGrE	0.032-0.64	0.019	[12]
FeSPCs/GluHD/GOx	-	2	[28]
CPE/$MnFe_2O_4$NPs/AuNPs	0.1-100	0.33	This work

To evaluate the repeatability of the applied strategy, five repeated measurements of flunitrazepam (25 μM) were carried out. The relative standard deviation (RSD) values were estimated to be 2.34 %. Furthermore, the reproducibility of the CPE/$MnFe_2O_4$NPs/AuNPs was checked with three CPE/$MnFe_2O_4$NPs/AuNPs in the analysis of 25 μM flunitrazepam at the same conditions. The RSD value of 2.11% was achieved using the obtained results indicating the satisfactory reproducibility of the sensor. The day-to-day stability of the sensor was monitored by measuring the anodic peak current response of 25 μM flunitrazepam over thirty days. The results showed the current decreased by a factor of less than 3.92% with a RSD of 2.29%. Moreover, investigation of the long term stability of the CPE/$MnFe_2O_4$NPs/AuNPs during one month reflects the acceptable stability of the sensor. A summary of the analytical figures of merit in the determination of flunitrazepam by this sensor is given in Table 2.

Table 2. The analytical figures of merit related to the proposed strategy for the determination of flunitrazepam

Figures of merit from the flunitrazepam sensor	Value
Linearity range (μM)	0.1-100
Sensitivity (μA/ μM)	0.7518
LOD (μM)	0.33
LOQ (μM)	0.90
Mean recovery for real samples (%)	100.12
Reproducibility (RSD%)	2.11
within-day precision (RSD%) n = 5	2.34
Day to day precision (RSD%) n = 5	2.29
Stability (day)	30

The anti-interference ability of the strategy towards flunitrazepam sensing in the presence of some probable interferences are an important parameter. Under the optimal experiment conditions, some organic compounds and mineral ions such as tartaric acid, cysteine, glucose, H_2O_2, Cl^-, Fe^{2+}, NO^{3-}, K^+ and Na^+ were separately tested in the measurement of 25 μM flunitrazepam in 0.04 M BR (pH= 8). Subsequently, the DPV responses of the flunitrazepam and the different probable interferences were evaluated (Table 3). The results indicated that none of the species caused a deviation on the peak current more than 5%, indicating all of them have no significant interfere in the flunitrazepam measurement.

Table 3. The effect some mineral ions and organic compounds in the measurement of 25 μM flunitrazepam on the CPE/$MnFe_2O_4$NPs/AuNPs

Excipients	Concentration (μM)	Signal change (%)
tartaric acid	1000	-1.30
glucose	1000	-1.53
H_2O_2	1000	-1.40
cysteine	1000	1.28
Cl^-	1000	0.43
Fe^{2+}	1000	0.20
NO^{3-}	1000	-0.61
K^+	1000	1.23
Na^+	1000	-1.00
SO_4^{2-}	1000	0.33
CO_3^-	1000	0.18

To evaluate the analytical application of the strategy, the DPV signals of the sensor in the absence and presence of other spiked drugs in the real samples were recorded. As listed in Table 4 in the human plasma the satisfactory results for the flunitrazepam detection are achieved. The results infer good agreement between the results of DPV by a RSD of 2.34 – 2.93% and recovery value of 97- 104%.

Table 4. Determination of the flunitrazepam in real samples with the CPE/$MnFe_2O_4$NPs/AuNPs sensor

Sample	Added (μM)	Found (μM)	Recovery (%)	RSD% (n = 6)
Human plasma	1.00	0.97	97.00	2.93
	5.00	5.24	104.0	2.64
	10.00	9.93	99.30	2.34

4. Conclusions

A high selective sensor based on the CPE modified with the $MnFe_2O_4$NPs and AuNPs for flunitrazepam sensing was fabricated. The $MnFe_2O_4$NPs and AuNPs as the unique modifier offered many advantages such as amplification of electron transfer and increase of surface area in flunitrazepam catalysis reaction. The sensor indicated a wide dynamic linear range, low detection limit, long-life storage as well as capability of flunitrazepam detection. Consequently, the strategy applied in this method with affordable features may be helpful in the generalization of entire miniaturized sensors in the detection of various targets in clinical studies in the real-sample.

Author's statement

Bahman Mohammadian Asiabar acquire various electrochemical data and synthesis and characterize $MnFe_2O_4$ and AuNPs, Dr. Mohammad Ali Karimi edited the manuscript and Prof.

Mehdi Rahimi-Nasrabadi and Dr. Hossein Tavallali provide all facility and investigate the different data and furthermore edited the manuscript.

References

[1] R.H. Schwartz, R. Milteer, M.A. LeBeau, Drug-facilitated sexual assault ('date rape'), Southern medical journal, 93 (2000) 558-561.
[2] F.P. Dubiela, M.G.M. de Oliveira, K.D.M. Moreira, J.N. Nobrega, S. Tufik, D.C. Hipólide, Learning deficits induced by sleep deprivation and recovery are not associated with altered [3H] muscimol and [3H] flunitrazepam binding, Brain research, 1037 (2005) 157-163.
[3] R.J. Dinis-Oliveira, T. Magalhães, Forensic toxicology in drug-facilitated sexual assault, Toxicology mechanisms and methods, 23 (2013) 471-478.
[4] P. D'Aloise, H. Chen, Rapid determination of flunitrazepam in alcoholic beverages by desorption electrospray ionization-mass spectrometry, Science & Justice, 52 (2012) 2-8.
[5] N. Leesakul, S. Pongampai, P. Kanatharana, P. Sudkeaw, Y. Tantirungrotechai, C. Buranachai, A new screening method for flunitrazepam in vodka and tequila by fluorescence spectroscopy, Luminescence, 28 (2013) 76-83.
[6] P.-H. Wang, C. Liu, W.-I. Tsay, J.-H. Li, R.H. Liu, T.-G. Wu, W.-J. Cheng, D.-L. Lin, T.-Y. Huang, C.-H. Chen, Improved screen and confirmation test of 7-aminoflunitrazepam in urine specimens for monitoring flunitrazepam (Rohypnol) exposure, Journal of analytical toxicology, 26 (2002) 411-418.
[7] L. Vlase, B. Kiss, F. Loghin, S.E. Leucuţa, Determination of flunitrazepam in human plasma and urine by HPLC with mass spectrometry detection, Journal of Liquid Chromatography & Related Technologies®, 31 (2008) 2442-2454.
[8] I. Deinl, C. Franzelius, L. Angermaier, G. Mahr, G. Machbert, On-line immunoaffinity extraction and HPLC analysis of flunitrazepam and its main metabolites in serum, Journal of analytical toxicology, 23 (1999) 598-602.
[9] S. Cui, S. Tan, G. Ouyang, J. Pawliszyn, Automated polyvinylidene difluoride hollow fiber liquid-phase microextraction of flunitrazepam in plasma and urine samples for gas chromatography/tandem mass spectrometry, Journal of Chromatography A, 1216 (2009) 2241-2247.
[10] S. Pirnay, S. Bouchonnet, F. Hervé, D. Libong, N. Milan, P. d'Athis, F. Baud, I. Ricordel, Development and validation of a gas chromatography–mass spectrometry method for the

simultaneous determination of buprenorphine, flunitrazepam and their metabolites in rat plasma: application to the pharmacokinetic study, Journal of Chromatography B, 807 (2004) 335-342.
[11] J.P. Smith, J.P. Metters, D.K. Kampouris, C. Lledo-Fernandez, O.B. Sutcliffe, C.E. Banks, Forensic electrochemistry: the electroanalytical sensing of Rohypnol®(flunitrazepam) using screen-printed graphite electrodes without recourse for electrode or sample pre-treatment, Analyst, 138 (2013) 6185-6191.
[12] E. Garcia-Gutierrez, C. Lledo-Fernandez, Electroanalytical sensing of Flunitrazepam based on screen printed graphene electrodes, Chemosensors, 1 (2013) 68-77.
[13] A. Hosseini, E. Sohouli, M. Gholami, A. Sobhani-Nasab, S.A. Mirhosseini, Electrochemical determination of ciprofloxacin using glassy carbon electrode modified with CoFe2o4-MWCNT, Analytical and Bioanalytical Electrochemistry, 11 (2019) 996-1008.
[14] E. Sohouli, A.H. Keihan, F. Shahdost-fard, E. Naghian, M.E. Plonska-Brzezinska, M. Rahimi-Nasrabadi, F. Ahmadi, A glassy carbon electrode modified with carbon nanoonions for electrochemical determination of fentanyl, Materials Science and Engineering: C, 110 (2020) 110684.
[15] E. Sohouli, F. Shahdost-Fard, M. Rahimi-Nasrabadi, M.E. Plonska-Brzezinska, F. Ahmadi, Introducing a novel nanocomposite consisting of nitrogen-doped carbon nano-onions and gold nanoparticles for the electrochemical sensor to measure acetaminophen, Journal of Electroanalytical Chemistry, (2020) 114309.
[16] T.H. Sanatkar, A. Khorshidi, E. Sohouli, J. Janczak, Synthesis, crystal structure, and characterization of two Cu (II) and Ni (II) complexes of a tetradentate N2O2 Schiff base ligand and their application in fabrication of a hydrazine electrochemical sensor, Inorganica Chimica Acta, (2020) 119537.
[17] E. Naghian, E.M. Khosrowshahi, E. Sohouli, F. Ahmadi, M. Rahimi-Nasrabadi, V. Safarifard, A new electrochemical sensor for the detection of fentanyl lethal drug by a screen-printed carbon electrode modified with the open-ended channels of Zn (ii)-MOF, New Journal of Chemistry, (2020).
[18] M. Gholami, M.A. Salmasi, E. Sohouli, B. Torabi, M.R. Sohrabi, M. Rahimi-Nasrabadi, A new nano biosensor for maitotoxin with high sensitivity and selectivity based fluorescence resonance energy transfer between carbon quantum dots and gold nanoparticles, Journal of Photochemistry and Photobiology A: Chemistry, (2020) 112523.
[19] E. Sohouli, E.M. Khosrowshahi, P. Radi, E. Naghian, M. Rahimi-Nasrabadi, F. Ahmadi, Electrochemical sensor based on modified methylcellulose by graphene oxide and Fe3O4 nanoparticles: Application in the analysis of uric acid content in urine, Journal of Electroanalytical Chemistry, (2020) 114503.
[20] C. Chikere, N. H. Faisal, P. K. T. Lin, C. Fernandez, Zinc oxide nanoparticles modified-carbon paste electrode used for the electrochemical determination of Gallic acid. In Journal of Physics: Conference Series, 1310 (2019) 012008.
[21] W. Yang, X. Zhou, N. Zheng, X. Li, Z. Yuan, Electrochemical biosensors utilizing the electron transfer of hemoglobin immobilized on cobalt-substituted ferrite nanoparticles–chitosan film, Electrochimica acta, 56 (2011) 6588-6592.
[22] S. Mirsadeghi, H. Zandavar, M. Rahimi, H.F. Tooski, H.R. Rajabi, M. Rahimi-Nasrabadi, E. Sohouli, B. Larijani, S.M. Pourmortazavi, Photocatalytic reduction of imatinib mesylate and imipenem on electrochemical synthesized Al2W3O12 nanoparticle: Optimization, investigation of electrocatalytic and antimicrobial activity, Colloids and Surfaces A: Physicochemical and Engineering Aspects, 586 (2020) 124254.

[23] E. Naghian, F. Shahdost-fard, E. Sohouli, V. Safarifard, M. Najafi, M. Rahimi-Nasrabadi, A. Sobhani-Nasab, Electrochemical determination of levodopa on a reduced graphene oxide paste electrode modified with a metal-organic framework, Microchemical Journal, (2020) 104888.
[24] B.A.H. Zaidan, E. Sohouli, S. Mazaheri, A Novel Capping Agent in Preparation and Characterization of CuAl2O4/CuO Nanocomposite and its Application for Electrochemical Detection of Dopamine, ANALYTICAL & BIOANALYTICAL ELECTROCHEMISTRY, 11 (2019) 108-122.
[25] A. Sobhani-Nasab, S. Behvandi, M.A. Karimi, E. Sohouli, M.S. Karimi, N. Gholipour, F. Ahmadi, M. Rahimi-Nasrabadi, Synergetic effect of graphene oxide and C3N4 as co-catalyst for enhanced photocatalytic performance of dyes on Yb2 (MoO4) 3/YbMoO4 nanocomposite, Ceramics International, 45 (2019) 17847-17858.
[26] E. Sohouli, M.S. Karimi, E.M. Khosrowshahi, M. Rahimi-Nasrabadi, F. Ahmadi, Fabrication of an electrochemical mesalazine sensor based on ZIF-67, Measurement, (2020) 108140.
[27] T.H. Sanatkar, A. Khorshidi, R. Yaghoubi, E. Sohouli, J. Shakeri, Stöber synthesis of salen-formaldehyde resin polymer-and carbon spheres with high nitrogen content and application of the corresponding Mn-containing carbon spheres as efficient electrocatalysts for the oxygen reduction reaction, RSC Advances, 10 (2020) 27575-27584.
[28] F. Tseliou, P. Pappas, K. Spyrou, J. Hrbac, M.I. Prodromidis, Lab-on-a-screen-printed electrochemical cell for drop-volume voltammetric screening of flunitrazepam in untreated, undiluted alcoholic and soft drinks, Biosensors and Bioelectronics, 132 (2019) 136-142.
[29] L. Hernández, P. Hernández, M.H. Blanco, E. Lorenzo, E. Alda, Determination of flunitrazepam by differential-pulse voltammetry using a bentonite-modified carbon paste electrode, Analyst, 113 (1988) 1719-1722.
[30] C. Lledo-Fernandez, P. Pollard, A. Romerosa, The Date rape Drug–Flunitrazepam-Electroanalytical Sensing Using Electrogenerated Chemiluminescence. International Journal of Electrochemical Science, 9 (2014) 227-237.
[29] I. Švancara, K. Vytřas, J. Barek, J. Zima, Carbon paste electrodes in modern electroanalysis, Critical Reviews in Analytical Chemistry, 31 (2001) 311-345.
[32] Y. Wang, H. Wei, J. Wang, J. Liu, J. Guo, X. Zhang, B.L. Weeks, T. Shen, S. Wei, Z. Guo, Electropolymerized polyaniline/manganese iron oxide hybrids with an enhanced color switching response and electrochemical energy storage, Journal of Materials Chemistry A, 3 (2015) 20778-20790.
[33] Y. Zeng, M. Yu, Y. Meng, P. Fang, X. Lu, Y. Tong, Iron-based supercapacitor electrodes: advances and challenges, Advanced Energy Materials, 6 (2016) 1601053.
[34] L. Geng, F. Yan, C. Dong, C. An, Design and regulation of novel MnFe2O4@ C nanowires as high performance electrode for supercapacitor, Nanomaterials, 9 (2019) 777.
[35] Y. Chen, Z. Shi, S. Li, J. Feng, B. Pang, L. Yu, W. Zhang, L. Dong, N, S-codoped graphene supports for Ag-MnFe2O4 nanoparticles with improved performance for oxygen reduction and oxygen evolution reactions, Journal of Electroanalytical Chemistry, 860 (2020) 113930.
[36] D.M. Fernandes, N. Silva, C. Pereira, C. Moura, J.M. Magalhães, B. Bachiller-Baeza, I. Rodríguez-Ramos, A. Guerrero-Ruiz, C. Delerue-Matos, C. Freire, MnFe2O4@ CNT-N as novel electrochemical nanosensor for determination of caffeine, acetaminophen and ascorbic acid, Sensors and Actuators B: Chemical, 218 (2015) 128-136.
[37] J. Zhang, C. Wang, Y. Niu, S. Li, R. Luo, Electrochemical sensor based on molecularly imprinted composite membrane of poly (o-aminothiophenol) with gold nanoparticles for sensitive

determination of herbicide simazine in environmental samples, Sensors and Actuators B: Chemical, 249 (2017) 747-755.
[3] A.P. Abbott, M. Azam, K.S. Ryder, S. Saleem, In situ electrochemical digital holographic microscopy; a study of metal electrodeposition in deep eutectic solvents, Analytical chemistry, 85 (2013) 6653-6660.
[39] Y. Zhu, D. Pan, X. Hu, H. Han, M. Lin, C. Wang, An electrochemical sensor based on reduced graphene oxide/gold nanoparticles modified electrode for determination of iron in coastal waters, Sensors and Actuators B: Chemical, 243 (2017) 1-7.
[40] S. Su, H. Sun, W. Cao, J. Chao, H. Peng, X. Zuo, L. Yuwen, C. Fan, L. Wang, Dual-target electrochemical biosensing based on DNA structural switching on gold nanoparticle-decorated MoS2 nanosheets, ACS applied materials & interfaces, 8 (2016) 6826-6833.
[41] N. Wang, M. Lin, H. Dai, H. Ma, Functionalized gold nanoparticles/reduced graphene oxide nanocomposites for ultrasensitive electrochemical sensing of mercury ions based on thymine–mercury–thymine structure, Biosensors and Bioelectronics, 79 (2016) 320-326.
[42] E. Tan, B. Erwin, S. Dames, K. Voelkerding, A. Niemz, Isothermal DNA amplification with gold nanosphere-based visual colorimetric readout for herpes simplex virus detection, Clinical chemistry, 53 (2007) 2017-2020.
[43] S.C. Nguyen, Q. Zhang, K. Manthiram, X. Ye, J.P. Lomont, C.B. Harris, H. Weller, A.P. Alivisatos, Study of heat transfer dynamics from gold nanorods to the environment via time-resolved infrared spectroscopy, Acs Nano, 10 (2016) 2144-2151.
[44] L. Scarabelli, M. Coronado-Puchau, J.J. Giner-Casares, J. Langer, L.M. Liz-Marzan, Monodisperse gold nanotriangles: size control, large-scale self-assembly, and performance in surface-enhanced Raman scattering, ACS nano, 8 (2014) 5833-5842.
[45] R. Omar, A.E. Naciri, S. Jradi, Y. Battie, J. Toufaily, H. Mortada, S. Akil, One-step synthesis of a monolayer of monodisperse gold nanocubes for SERS substrates, Journal of Materials Chemistry C, 5 (2017) 10813-10821.
[46] S. Gong, W. Schwalb, Y. Wang, Y. Chen, Y. Tang, J. Si, B. Shirinzadeh, W. Cheng, A wearable and highly sensitive pressure sensor with ultrathin gold nanowires, Nature communications, 5 (2014) 1-8.
[47] E.K. Beloglazkina, A.G. Majouga, R.B. Romashkina, N.V. Zyk, N.S. Zefirov, Gold nanoparticles modified with coordination compounds of metals: synthesis and application, Russian Chemical Reviews, 81 (2012) 65.
[48] C.M. Cobley, J. Chen, E.C. Cho, L.V. Wang, Y. Xia, Gold nanostructures: a class of multifunctional materials for biomedical applications, Chemical Society Reviews, 40 (2011) 44-56.
[49] J. Huang, J. Tian, Y. Zhao, S. Zhao, Ag/Au nanoparticles coated graphene electrochemical sensor for ultrasensitive analysis of carcinoembryonic antigen in clinical immunoassay, Sensors and Actuators B: Chemical, 206 (2015) 570-576.
[50] M. George, A.M. John, S.S. Nair, P. Joy, M. Anantharaman, Finite size effects on the structural and magnetic properties of sol–gel synthesized NiFe2O4 powders, Journal of Magnetism and Magnetic Materials, 302 (2006) 190-195.
[51] J. Li, H. Xie, L. Chen, A sensitive hydrazine electrochemical sensor based on electrodeposition of gold nanoparticles on choline film modified glassy carbon electrode, Sensors and Actuators B: Chemical, 153 (2011) 239-245.

[52] S. Ghasemi, S. R. Hosseini, F. Mousavi, Electrophoretic deposition of graphene nanosheets: A suitable method for fabrication of silver-graphene counter electrode for dye-sensitized solar cell. Colloids and Surfaces A: Physicochemical and Engineering Aspects, 520 (2017) 477-487.
[53] F. Mousavi, A. A. Taherpour, A carbon nanotube-iron (III) oxide nanocomposite as a cathode in dye-sensitized solar cells: Computational modeling and electrochemical investigations. Electrochimica Acta, 318 (2019) 617-624.
[54] K. Adib, M. Rahimi-Nasrabadi, Z. Rezvani, S.M. Pourmortazavi, F. Ahmadi, H.R. Naderi, M.R. Ganjali, Facile chemical synthesis of cobalt tungstates nanoparticles as high performance supercapacitor, Journal of Materials Science: Materials in Electronics, 27 (2016) 4541-4550.
[55] F. Feizi, M. Shamsipur, A. Barati, M. B. Gholivand, F. Mousavi, Chiral recognition and quantitative analysis of tyrosine enantiomers using L-cysteine capped CdTe quantum dots: Circular dichroism, fluorescence, and theoretical calculation studies. Microchemical Journal, 158 (2020) 105168.
[56] F. Mousavi, M. Shamsipur, A. A. Taherpour, A. Pashabadi, A rhodium-decorated carbon nanotube cathode material in the dye-sensitized solar cell: Conversion efficiency reached to 11%. Electrochimica Acta, 308 (2019) 373-383.

Highlights

- flunitrazepam is used as a strong sedative for the treatment of severe insomnia.
- An electrochemical sensor based on the clever combination of the $MnFe_2O_4$ and AuNPs is fabricated for the first time.
- A novel electrochemical sensor based CPE/$MnFe_2O_4$NPs is presented for analysis of flunitrazepam.
- A linear range of 0.1-100 μM was achieved by the sensor in clinical sample.